Predicting sensory evaluation indices of Cheddar cheese texture by fluorescence fingerprint measurement coupled with an optical fibre

Title

Predicting sensory evaluation indices of Cheddar cheese texture by fluorescence fingerprint measurement coupled with an optical fiber

Authors

Akira Chiba[a, b], Mito Kokawa[c,*], Mizuki Tsuta[d], Setsuko Todoriki[c, d]

Affiliations and addresses

[a] *Food Research & Development Institute, R&D Division, Morinaga Milk Industry Co., Ltd., 5-1-83 Higashihara, Zama, Kanagawa 252-8583, Japan*

[b] *Graduate School of Life and Environmental Sciences, University of Tsukuba, 1-1-1 Ten-noudai, Tsukuba, Ibaraki 305-8577, Japan*

[c] *Faculty of Life and Environmental Sciences, University of Tsukuba, 1-1-1 Ten-noudai, Tsukuba, Ibaraki 305-8577, Japan*

[d] *Food Research Institute, National Agriculture and Food Research Organization, 2-1-12 Kan-nondai, Tsukuba, Ibaraki 305-8642, Japan*

*Corresponding author. Tel: +81 29 853 4659

E-mail address: kokawa.mito.ke@u.tsukuba.ac.jp (M. Kokawa)

ABSTRACT

A fluorescence fingerprint (FF) was used to develop a quick and non-contact practical method for predicting the sensory evaluation index of cheese texture (cheese body measurement). A partial least-squares (PLS) model was constructed from FF data and cheese body measurements of Cheddar cheeses. The cheese body measurement was successfully predicted by the PLS model with a coefficient of determination for calibration of 0.800. Notably, the reproducibility of the prediction value and the model accuracy were comparable to those of a conventional FF model despite the non-contact measurement. By exploring the variable importance in projection (VIP) and selectivity ratio (SR) of the PLS model, the fluorescence likely corresponding to oxidized lipids, Maillard reaction products, and compounds of proteins and amino acids with oxidized lipids was found to increase in intensity with the progress of ripening. This suggests that the fluorescence of these compounds contributes to the accuracy of the PLS model.

1. Introduction

The composition (fat, moisture, and intact casein) and maturity of natural cheese as a raw material for processed cheese has a significant impact on the product quality and stability (Guinee, Caric, & Kalab, 2004; Kapoor & Metzger, 2008; Tamime, 2011). Generally, young cheese is used to produce hard processed cheese, whereas aged cheese is used to produce soft processed cheese. For example, block-type processed cheeses that are easy to slice and are elastic require a young cheese, whereas spread-type processed cheeses are primarily based on cheese with medium maturity. However, as natural cheese starts to mature immediately after manufacturing, the maturity of individual natural cheeses used to make processed cheese will differ. Therefore, to achieve products with sufficient uniformity, the blending ratio must be adjusted daily.

Processed cheese has numerous advantages including 1) a long shelf-life; 2) the characteristics of multiple natural cheeses through which, with additional seasoning, variations in the taste can be enhanced; 3) a mild taste, making it palatable for children and people who may not be familiar with natural cheese; 4) an easily modified shape and readily adjustable texture (elasticity, hardness, spreadability, and ease of slicing); and 5) high suitability for cooking (flow, ease of browning, and viscosity).

Assessment of the texture of cheese based on detailed measurements represents an active area of research. In particular, the relationship between physical properties and texture evaluated through instrumental measurements and sensory evaluation (Drake, Gerard, Truong, & Daubert, 1999; Foegeding, Brown, Drake, & Daubert, 2003; Guinee & Kilcawley, 2004; Lee, Imoto, & Rha, 1978; Morita et al., 2015; O'Callaghan & Guinee, 2004; Xiong, Meullenet, Hankins, & Chung, 2002) constitutes a primary area of interest. However, only a few measurement methods are actively used by processed cheese manufacturers to evaluate natural cheese as raw materials. An example of such methods currently on the market includes “Caseus Pro™” (Gold Peg International, Inc., Braeside, Australia). This is because the

59 pretreatment process for evaluation and instrumental measurement is complex, the measurement results
60 cannot be directly related to traditional sensory evaluation results, and the number of samples required for
61 appropriate evaluation is excessively large. Therefore, in general, sensory evaluation approaches are faster.
62 Individual processed cheese manufacturers continue to use traditional sensory evaluation or only employ
63 instrumental measurement data directly, with each company using its own methods. For example, an index
64 termed “cheese body measurement” is used for the sensory evaluation of physical properties. The cheese
65 body measurement is an index of the physical maturity determined by trained experts that is based on the
66 physical sensation of crumbling a piece of cheese between the fingers. This index varies between 1 and 10,
67 where 10 points indicates a strong body (young texture without maturing) whereas 1 point indicates a
68 weak body (matured texture), and is likely to vary significantly among cheese manufacturers
69 (Mizuno & Ichihashi, 2007; Muir, 2010; Nakazawa & Hosono, 1989).
70 Alternatively, methods have been developed that utilize mid-infrared light, near-infrared light,
71 fluorescence, and Raman spectroscopy to predict the components and physical properties of food, which
72 are used as quick measurement methods (Nawrocka & Lamorska, 2013). As fluorescence and
73 near-infrared spectra can be measured without sample pretreatment, these spectroscopic methods exhibit
74 high potential for industrial use. In particular, fluorescence spectroscopy measures the emission spectrum
75 instead of the absorption spectrum and demonstrates high sensitivity compared to that of near-infrared
76 light (Karoui, Mazerolles, & Dufour, 2003; Kulmyrzaev, Karoui, De Baerdemaeker, & Dufour, 2007).
77 Fluorescent compounds are sensitive to their surrounding environment (e.g., temperature, ionic
78 concentration, pH, and polarity of solution); moreover, fluorescence spectroscopy measurements can be
79 rapidly performed (Dufour, 2011). In addition, some investigations have been performed involving the
80 measurement of cheese using fluorescence spectroscopy (Andersen & Mortensen, 2008; Christensen,
81 Nørgaard, Bro, & Engelsen, 2006; Dufour, 2011; Karoui & Blecker, 2011). Furthermore, with the
82 development of information processing technologies in recent years, fluorescence spectroscopy

83 measurements allow the rapid acquisition of emission spectra from excitation light with a continuous
84 wavelength, such as in the form of an excitation-emission matrix (EEM), also known as a fluorescence
85 fingerprint (FF).
86 The FF has an advantage over conventional fluorescence spectra because it includes emission spectra
87 excited at many different excitation wavelengths. Thus, FF yields much more information as compared
88 with the study of conventional single or double excitation wavelengths, and has the potential to estimate
89 phenomena with high accuracy. This approach is used as a measurement method by which a large amount
90 of information can be acquired and processed (Airado-Rodríguez, Galeano-Díaz, Durán-Merás, & Wold,
91 2009). A FF targets not only the peak intensity of the fluorescence signal but also other wavelength ranges
92 in which the fluorescence signal is weak. A model can then be constructed that only extracts necessary
93 information. There are several instruments that can derive predictions based on fluorescence and a FF.
94 Although a few analytical cases have been examined and numerous discussions have been conducted
95 regarding the predictive accuracy obtained using these techniques, to our knowledge no reports are yet
96 available of a detailed prediction model based on the contributing wavelength range or other factors
97 (Lacotte et al., 2015; Liu, Sajith Babu, Coutouly, Allouche, & Amamcharla, 2016). However, there have
98 been some cases of FFs being applied to study food (Sádecká & Tóthová, 2007) including dairy products
99 containing cheese (Andersen & Mortensen, 2008; Boubellouta & Dufour, 2008; Christensen, Povlsen, &
100 Sørensen, 2003).
101 Although there have been some studies that predicted cheese texture and physical properties using
102 fluorescence spectroscopy (Garimella Purna, Prow, & Metzger, 2005; Karoui et al., 2003; Karoui &
103 Dufour, 2006; Kulmyrzaev et al., 2005; Lebecque, Laguet, Devaux, & Dufour, 2001; Ozbekova &
104 Kulmyrzaev, 2017), their predictions were based on the fluorescence of a limited number of entities such
105 as tryptophan and vitamin A. Moreover, the emission spectra were measured by using only single or
106 double excitation wavelengths, with the primary purpose being to analyze the correlation between the

107 peak intensity and components or textures. Recently, Kokawa et al. (2015) showed that a FF can predict
108 indices of cheese maturation. They predicted the maturation time and some chemical analysis values,
109 such as the proteolysis index (the ratio of water-soluble nitrogen content to total nitrogen content) and
110 total free amino acid content, from FFs. They also demonstrated that the FF constitutes an effective tool
111 for capturing changes in cheese through maturation. However, their method of measurement still requires
112 the preparation of samples with a shape that fits the cell of the fluorescence spectrophotometer. In
113 addition, there have been no studies where a FF has been used to predict the cheese body measurement,
114 the index of sensory evaluation for cheese texture, for the raw materials of processed cheese.
115 In this study, our aim was to develop a rapid method for predicting the cheese body measurement
116 using a FF, regardless of the experience level of the user. Then, we attempted to develop a method for
117 non-contact prediction of the cheese body measurement by exploiting the optical fiber unit in a
118 fluorescence spectrophotometer. In consideration of the practicality for industrial use, we have chosen a
119 non-contact measurement using a fiber optics unit to eliminate the pretreatment of the sample. Although
120 some reports are available in areas other than dairy research, no examples yet exist of application of this
121 method to cheese texture. By removing the sample pretreatment step, measurement of the FF was easily
122 achieved. Non-contact measurement of changes in the cheese with maturation will thus be faster than
123 traditional methods, rendering this method useful for processed cheese manufacturers.
124

2. Materials and Methods

2.1. Cheese samples

Ten Australian Cheddar cheese samples were used for measurements. We performed three measurements and evaluations over time and obtained the results for a total of 30 samples. These cheese samples were matured at −2 °C, 5 °C, 10 °C, and 15 °C to achieve differences in the cheese body measurement. Each cheese sample was divided into blocks for FF measurement and cheese body measurement evaluation. Cheese samples were also analyzed for moisture (ISO/IDF 4: 2004a), fat (ISO/IDF 5: 2004b), and protein (ISO/IDF 185: 2002). The pH was measured by insertion of a pH probe (D-54, Horiba, Kyoto, Japan) into the ground cheese sample.

2.2. Evaluation of cheese body measurement

The cheese body measurement was evaluated by five trained experts in consultation after adjusting the temperature of the cheese to 5 °C. The maximum score for the cheese body measurement was 10, corresponding to the strongest texture (young texture), with a score of 1 corresponding to the weakest texture (matured texture). The cheese body measurement and FF were measured on the same day or on consecutive days so that there was no difference in maturation.

2.3. FF measurement

To measure the FF of cheese, we used a fluorescence spectrophotometer (F-7000, Hitachi High-Technologies Corporation, Tokyo, Japan) and an optical fiber unit (5J0-0114-F-7000, Hitachi High-Technologies) (Mita Mala et al., 2016). The cheese samples subjected to FF measurement were adjusted to 20 °C and cut into blocks of 3 cm × 3 cm × 6 cm. The side of the cheese samples was selected randomly and was cut immediately prior to FF measurement, and measurements were taken on a fresh surface each time. The samples were then placed on a stage with a fixed fiber unit. During measurement,

149 external light was excluded from the sample using an enclosure. The measurement conditions for the FF
150 were an excitation wavelength of 200–500 nm, an emission wavelength of 200–800 nm, and a wavelength
151 interval of 5 nm. The slit width of the monochromator was 10 nm for both excitation and emission
152 wavelengths. A photomultiplier voltage of 500 V was used and the scan speed was 60,000 nm min^{-1}. The
153 distance between the probe tip of the fiber unit and the cheese sample was 5 mm, and the measurement
154 was made without contact. Three replicates were measured for each cheese sample.
155
156 *2.4. PLS model for prediction of cheese body measurement*
157 To predict the cheese body measurement from the FF measurements, a partial least-squares (PLS)
158 regression model was constructed. For the multivariate analysis, MATLAB (R2016a) software
159 (MathWorks Inc., Natick, MA, USA) and PLS Toolbox version 8.1.1 (Eigenvector Inc., Manson, WA
160 USA) were used. FF data were preprocessed using the method of Yoshimura et al. (2014). First, as
161 fluorescence constitutes an emission with wavelengths longer than the excitation wavelength, all data with
162 emission wavelengths shorter than the excitation wavelengths were removed. Next, the primary light and
163 the secondary and tertiary scattered lights, which comprise lights with the emission wavelengths at twice
164 and three times the excitation wavelength (Fujita, Tsuta, Kokawa, & Sugiyama, 2010), respectively, were
165 removed. Finally, excitation wavelengths shorter than 230 nm were removed because they contained
166 significant noise. The remaining data were a combination of 3,869 excitation wavelengths and emission
167 wavelengths.
168 In total, we performed PLS regression analysis using 90 (three replicates × 10 samples × three
169 evaluation periods) evaluation results for FF data. The cheese body measurement was measured for 30
170 samples (10 samples × three evaluation periods). First, the data were divided into calibration and
171 validation sets (2:1). Specifically, the samples were aligned in order of measurement and measurements
172 for every third sample were allocated to the validation set and those for the rest were allocated to the

calibration set. Next, a cross-validation model using the calibration set was employed to determine the optimum pretreatment and number of latent variables (LVs). Three preprocessing methods were used for the FF data: mean centering, normalization followed by mean centering, and autoscaling. The data were normalized so that the area underneath each spectrum was equal to 1. In autoscaling, each wavelength was scaled to 0.0 mean and unit variance. The number of LVs was determined using a PLS Toolbox algorithm that determines the descending point known as the "knee" in a scree plot (Henry, Park, & Spiegelman, 1999). Next, the selected LVs and pretreatment were used to prepare a model based on the calibration set. Furthermore, we applied this model to the validation set data to confirm the accuracy of the prediction. The accuracy of the prediction model was evaluated using the coefficients of determination of cross-validation (R^2CV) and prediction (R^2P) and the root-mean-square errors of cross-validation (RMSECV) and prediction (RMSEP). In addition, we calculated the variable importance in projection (VIP), the selectivity ratio (SR), and the regression vector for the model and determined the wavelength range that mainly contributes to the model.

3. Results and Discussion

3.1. Fluorescence fingerprints and cheese compositions

Figure 1 shows the mean FF for the cheese samples. An emission peak was observed in the excitation wavelength range of 290–305 nm and the emission wavelength range of 320–350 nm. This peak had a fluorescence intensity of 6131 (a.u.) and has been determined to correspond to aromatic amino acids including tryptophan (Andersen, Vishart, & Holm, 2005; Andersen & Mortensen, 2008; Mazerolles et al., 2001). In addition, the intensity was high (1201 (a.u.)) at the excitation wavelength of 320 nm and emission wavelength of 400 nm, which are likely the wavelengths of vitamin A. We focused on the peak at ex320/em400 because it has been examined in many previous reports. Fluorescence measurements for milk (Boubellouta & Dufour, 2008; Dufour & Riaublanc, 1997), soft cheese (Herbert et al., 2000), semi-hard cheese (Karoui, Dufour, & De Baerdemaeker, 2006), and processed cheese (Christensen et al., 2003) have been previously reported. The peak at the excitation wavelength of 300 nm and the emission wavelength of 680 nm represents the second-order light of the excitation wavelength of 300 nm and the emission wavelength of 335 nm, which appears owing to the light dispersion mechanism of the monochrometer (i.e., the same mechanism that creates the second-order scattering light). In the FF data, similar peaks were detected to those in Kokawa et al. (2015); thus, we confirmed that a non-contact FF could be obtained for cheese using an optical fiber.

Table 1 shows the age, composition and pH of 10 sample cheeses. It was confirmed that there was little difference in composition and pH between samples.

3.2. PLS prediction model

Table 2 shows the LVs and prediction accuracy of the PLS regression model for each pretreatment. Before performing the PLS regression analysis, four pretreatments were evaluated to optimize the model in terms of R^2CV and RMSECV. The present model that used the mean center and normalization followed

by the mean center as a pretreatment exhibited a similar level of accuracy with R^2CV of 0.787 and RMSECV of 0.456. “Normalize” constitutes the pretreatment whereby the sum of the luminance is normalized to be 1. This pretreatment can reduce the variation caused by differences in overall brightness (although the spectral shapes are the same). In this study, it made no difference in precision whether “normalize"’ was performed or not; there is thus a possibility that such variation was small. The “autoscale” and “normalize + autoscale” were not adopted because the precision was low.

Figure 2 (the calibration set) and Fig. 3 (the validation set) show the relationship between the cheese body measurement predicted from the FF using the optical fiber unit and the actually evaluated cheese body measurement. The prediction model was developed with three LVs using the pretreatment of the mean center. In the validation set, we obtained a strong correlation ($R^2P = 0.826$) and small prediction error (RMSEP = 0.436). Additionally, the relative standard deviation (RSD) of the body value predicted by FFs in the three replicates was 0.21% minimum and 5.4% maximum. The average of RSD with three replicates in all 30 samples was 1.6%. These values show that this method can be applied repeatedly with just 1–2% variation and has high reproducibility. The results shown in Figs. 2 and 3 indicate that 1) the FF can predict the cheese body measurement although attention is required for cheese body measurements of around six, and 2) using the optical fiber unit, the cheese body measurement can be predicted through non-contact measurement.

The evaluation of cheese body measurements by the experts in this study often resulted in cheese body measurements of around six; thus, the distribution of the evaluation data was unequal. This is likely to have reduced the prediction accuracy. As the predicted cheese body measurements of around six have a higher variation than that of other cheese body measurements, the handling of results close to this value requires attention. To further improve the accuracy, the number of samples can be increased, or samples should be selected so that the distribution of cheese body measurements across the scoring range is even.

3.3. VIP and SR scores of the PLSR model plotted using FF contour representation

Figure 4 shows the VIP and SR scores as a contour map to identify the range of wavelengths that contributes to the PLS regression model. Two wavelength ranges with high VIP scores were identified (Fig. 4a). Wavelengths with VIP scores of 1 or higher are known to be important variables in the model (Mehmood, Liland, Snipen, & Sæbø, 2012). The highest VIP score (69.9) was observed in the wavelength ranges with an excitation wavelength of 305 nm and an emission wavelength of 340 nm. Subsequently, the wavelength ranges with an excitation wavelength of 340 nm and an emission wavelength of 400 nm also showed high VIP value (VIP score = 15.9). The VIP value of the wavelength ranges with an excitation wavelength of 300 nm and an emission wavelength of 680 nm was also high, but we did not pursue this range because it represented the second-order light of an excitation wavelength of 300 nm and an emission wavelength of 340 nm. As has been previously reported, the excitation wavelength of 305 nm and emission wavelength of 340 nm were considered to represent tryptophan and aromatic amino acids (Andersen et al., 2005; Andersen & Mortensen, 2008; Mazerolles et al., 2001).

As an alternative, Fig. 4b shows a contour map of the SR scores. SR scores provide a numerical evaluation of the utility of each variable in a regression model. The SR scores can be used to build a model with even higher accuracy by excluding wavelength ranges with low SR scores and selecting wavelengths with only high SR scores (Rajalahti et al., 2009). In the present study, we used the F-test (95%) standard to select wavelength ranges with a large contribution (Farrés, Platikanov, Tsakovski, & Tauler, 2015). The SR score of the F-test (95%) was 1.55. Wavelength ranges with a SR score above this value (SR score > 1.55) included the excitation wavelengths of 335–445 nm and emission wavelengths of 370–520 nm. In these ranges, the excitation wavelength of 385 nm and emission wavelength of 460 nm comprised the peak wavelengths. The peak SR score for these excitation-emission wavelengths was 7.11. The SR score of the excitation wavelength of 350 nm and the emission wavelength of 770 nm was also high, but this wavelength range was also not further pursued because it represented second-order light of

259 the excitation wavelength of 340 nm and the emission wavelength of 400 nm.

260 As VIP scores only take positive values, we used the regression coefficient (regression vector) shown
261 in Fig. 4c to determine whether the wavelengths correlated positively or negatively with the cheese body
262 measurements. The regression vector for each VIP peak revealed that the value was positive at the
263 excitation wavelength of 305 nm and emission wavelength of 340 nm and negative at the excitation
264 wavelength of 340 nm and emission wavelength of 400 nm. This suggests that the fluorescence intensity
265 of the former wavelengths decreases as the cheese body measurement decreases, whereas that of the latter
266 wavelengths increases.

267 Figure 5a shows the emission spectra of all samples at an excitation wavelength of 340 nm. The peak
268 intensity around the emission wavelength of 400 nm increased as the cheese body measurement
269 decreased; the correlation coefficient of the fluorescence at the excitation wavelength of 340 nm and
270 emission wavelength of 400 nm with the cheese body measurement was −0.77. The fluorescence intensity
271 of each fluorophore reflects how they are metabolized during cheese maturation. In this study, we
272 considered that the wavelength range of excitation wavelength of 340 nm and emission wavelength of 400
273 nm, which exhibited high correlation with cheese body measurement, was related to substances that
274 increased during cheese maturation.

275 Numerous investigations have focused on the range near the excitation wavelength of 340 nm and the
276 emission wavelength of 400 nm. Stapelfeldt & Skibsted (1994) reported that in a model system of dairy
277 products and β-lactoglobulin, accumulated secondary lipid oxidation products emit fluorescence at
278 excitation wavelengths of 350 nm and emission wavelength of 410 nm. Morales, Romero, &
279 Jiménez-Pérez (1996) monitored the fluorescence of Maillard reaction products during the thermal
280 processing of a model system using milk and dairy products at an excitation wavelength of 347 nm and
281 emission wavelength of 415 nm. These model system studies demonstrated that oxidized lipid and
282 Maillard reaction products of milk and dairy products could be monitored via their fluorescence in the

range near the excitation wavelength of 340 nm and the emission wavelength of 400 nm. In addition, Kokawa et al. (2015) selected peaks at an excitation wavelength of 345 nm and emission wavelength of 400 nm as the wavelength values with a large contribution to the PLS regression model in the FF of cheese maturation indices, which suggested that oxidized lipids and Maillard reaction products are present in Cheddar cheese. These are thus considered to be the same substances as measured in the present study, as we also focused on these wavelengths based on the VIP values in this study. Notably, although Maillard reactions do not proceed actively in hard and semi hard cheeses, studies using Manchego (Corzo, Villamiel, Arias, Jiménez-Pérez, & Morales, 2000), Cheddar, Gouda and Emmental (Schwietzke, Schwarzenbolz, & Henle, 2009), Harzer and Gouda cheeses (Spanneberg, Salzwedel, & Glomb, 2012) have been reported that the Maillard reaction proceeded along with cheese maturation of these cheeses. These studies measured Maillard reaction products in young and matured cheese using high performance liquid chromatography analysis. As the amount of Maillard reaction products tends to increase during cheese maturation, they are likely to show correlation with the cheese body measurement.

Figure 5b shows the emission spectra at an excitation wavelength of 385 nm, where the SR score was the highest. The maximum wavelength of the fluorescence was between 500 and 550 nm, although multiple peaks were also confirmed around 460 nm. The fluorescence peaks around 460 nm increased in intensity as the cheese body measurement decreased, with the correlation coefficient between the cheese body measurement and the fluorescence intensity at an excitation wavelength of 385 nm and emission wavelength of 460 nm being −0.79.

The fluorescence constituents most commonly reported in this range are the reaction products between amino acids, proteins, and oxidized lipids. Kikugawa, Takayanagi, & Watanabe (1985) reported that the reaction product of malondialdehyde (MDA) and lysine monomer generated by lipid oxidation has a maximum excitation wavelength of 395 nm and maximum emission wavelength of 466–470 nm. In addition, they reported that the reaction product of MDA and a model protein, polylysine, has a maximum

307 excitation wavelength of 398 nm and maximum emission wavelength of 470 nm. The same group
308 (Kikugawa & Beppu, 1987) reported that with the generation of fluorescent substances through lipid
309 oxidation in tissues and cells, the reaction of MDA and primary amines in the presence of monofunctional
310 aldehydes is promoted, generating fluorescent 1,4-disubstituted 1,4-dihydropyridine-3,5-dicarbaldehydes.
311 The maximum excitation wavelength of the reaction products was 386–403 nm and maximum emission
312 wavelength was 444–465 nm. Yamaki, Kato, & Kikugawa (1992) reported that the reaction product of
313 hexenal and glycine ethyl had a maximum excitation wavelength of 392 nm and maximum emission
314 wavelength of 455 nm. Veberg, Vogt, & Wold (2006) fixed the excitation wavelength at 382 nm and
315 reported the fluorescence of the reaction product of oxidized lipids (aldehydes) and amino acids. They
316 found that the reaction product of lysine and 2-hexenal has a maximum fluorescence at 471 nm, whereas
317 the reaction product of lysine and 2,4-heptadienal has a maximum fluorescence at 472 nm. The reaction
318 product of malondialdehyde and glycine shows maximum fluorescence at 465–469 nm, whereas the
319 reaction with lysine shows maximum fluorescence at 467–469 nm (both with an excitation wavelength of
320 382 nm). Furthermore, they showed that the fluorescence is generated at a temperature of 4 °C under
321 refrigeration. The same group (Veberg, Olsen, Nilsen, & Wold, 2007) also reported that the maximum
322 emission wavelength for oxidized lipids in butter during light irradiation was 465–470 nm, and indicated
323 that the peak emission of the oxidized lipids occurs around 470 nm regardless of the type of food (e.g.,
324 salted cod, turkey, chicken meat, or salmon pâte). In the present experiment, we did not use any
325 irradiation during storage; however, oxidized lipids may be generated during long-term storage.
326 In comparison, lumichrome, generated by the photo-oxidation of riboflavin, has an
327 excitation-emission peak near the same range; however, the peak wavelengths were an excitation
328 wavelength of 360 nm and emission wavelength of 450 nm in the model system (Fox & Thayer, 1998) but
329 an excitation wavelength of 370 nm and emission wavelength of 430 nm in yogurt (Christensen, Becker,
330 & Frederiksen, 2005). In addition to this discrepancy, the low contribution of riboflavin fluorescence to

331 the model also suggests that the effect of lumichrome was small. If lumichrome had high relevance with
332 the accuracy of the PLS model, riboflavin should also show high relevance. However, the wavelength
333 area corresponding to riboflavin fluorescence did not show high contribution to the PLS regression
334 model.

335 Figure 5c shows the emission spectra at an excitation wavelength of 305 nm, at which there is a peak
336 in VIP. Peaks near the emission wavelength of 340 nm showed high fluorescence intensity; however, the
337 correlation with the cheese body measurement was low, with the correlation coefficient of the
338 fluorescence intensity with the cheese body measurement at an excitation wavelength of 305 nm and
339 emission wavelength of 340 nm being 0.05. Although tryptophan and aromatic amino acids represented
340 by these peak wavelengths have been used to predict the parameters of dairy products including cheese
341 (Andersen & Mortensen, 2008), in the present study, the correlation coefficient was low and the
342 contribution to the PLS regression model was low. This wavelength range has strong fluorescence
343 intensity and captures changes well, but by performing a comprehensive analysis such as on the FF,
344 changes during cheese maturation will have even higher correlation, which will allow the identification of
345 the range of wavelengths contributing to the accuracy of the PLS regression model. We also suggest that
346 in future studies, it should be possible to confirm the substances showing high correlation with the
347 changes in the cheese body measurement by performing chemical analysis (e.g., extraction and high
348 performance liquid chromatography) to quantify the substances, and then comparing the relative quantity
349 of the substance of interest with the cheese body measurement.
350

351 **4. Conclusion**

352 We showed that non-contact FF measurements using an optical fiber probe can be used to predict the
353 cheese body measurement of Cheddar cheese. Compared with conventional fluorescence measurements
354 in a photometer chamber using cells to hold the sample, it was possible to develop a more practical

355 method. The predictive ability of the model was reliable with a strong correlation (R2P = 0.826) and small
356 prediction error (RMSEP = 0.436). Moreover, the average RSD of the three replicates in all 30 samples
357 was 1.6%. These values show that this method can be applied repeatedly with only 1–2% variation and has
358 high reproducibility. Despite the non-contact FF measurement, it was confirmed that the accuracy of this
359 prediction model is equivalent to that of previous studies. However, as the predicted values for cheese
360 body measurements of around six show large variation, it is necessary to improve the accuracy by using
361 data that reflect a more uniform distribution of cheese body measurements.
362 The wavelength ranges of oxidized lipids and Maillard reaction products (excitation wavelength of
363 340 nm and emission wavelength of 400 nm), which were assumed to make a large contribution to the
364 prediction of indices of cheese maturation (maturation time, proteolysis index, and free amino acid
365 content) in previous reports, were shown to also make a large contribution to the present cheese body
366 measurement prediction model.
367 By exploring the SR scores, we discovered a new wavelength range with a large contribution to the
368 PLS regression model. These wavelengths were considered to correspond to oxidized lipids or to
369 compounds of proteins and amino acids with oxidized lipids. Additional studies are necessary to confirm
370 whether these products are responsible for these new wavelength changes, such as by comparing the
371 results of quantification of these product contents with the FF measurements. Thus, our results suggest that
372 the rapid and simple non-contact FF method developed herein for predicting the cheese body measurement
373 may be suitable for industrial application to enhance the quality and reliability of processed cheese
374 production.
375
376 Funding: This research did not receive any specific grant from funding agencies in the public, commercial,
377 or not-for-profit sectors.
378

379 **References**

380

381 Airado-Rodríguez, D., Galeano-Díaz, T., Durán-Merás, I., & Wold, J. P. (2009). Usefulness of
382 fluorescence excitation-emission matrices in combination with PARAFAC, as fingerprints of red
383 wines. *Journal of Agricultural and Food Chemistry, 57*, 1711-1720.
384 Andersen, C. M., & Mortensen, G. (2008). Fluorescence spectroscopy: a rapid tool for analyzing dairy
385 products. *Journal of Agricultural and Food Chemistry, 56*, 720-729.
386 Andersen, C. M., Vishart, M., & Holm, V. K. (2005). Application of fluorescence spectroscopy in the
387 evaluation of light-induced oxidation in cheese. *Journal of Agricultural and Food Chemistry, 53*,
388 9985-9992.
389 Boubellouta, T., & Dufour, E. (2008). Effects of mild heating and acidification on the molecular structure
390 of milk components as investigated by synchronous front-face fluorescence spectroscopy
391 coupled with parallel factor analysis. *Applied Spectroscopy, 62*, 490-496.
392 Christensen, J., Becker, E. M., & Frederiksen, C. S. (2005). Fluorescence spectroscopy and PARAFAC in
393 the analysis of yogurt. *Chemometrics and Intelligent Laboratory Systems, 75*, 201-208.
394 Christensen, J., Nørgaard, L., Bro, R., & Engelsen, S. B. (2006). Multivariate autofluorescence of intact
395 food systems. *Chemical Reviews, 106*, 1979-1994.
396 Christensen, J., Povlsen, V. T., & Sørensen, J. (2003). Application of fluorescence spectroscopy and
397 chemometrics in the evaluation of processed cheese during storage. *Journal of Dairy Science, 86*,
398 1101-1107.
399 Corzo, N., Villamiel, M., Arias, M., Jiménez-Pérez, S., & Morales, F. J. (2000). The Maillard reaction
400 during the ripening of Manchego cheese. *Food Chemistry,* 71, 255-258.
401 Drake, M. A., Gerard, P. D., Truong, V. D., & Daubert, C. R. (1999). Relationship between instrumental
402 and sensory measurements of cheese texture. *Journal of Texture Studies, 30*, 451-476.

403 Dufour, E. (2011). Recent advances in the analysis of dairy product quality using methods based on the
404 interactions of light with matter. *International Journal of Dairy Technology, 64*, 153-165.
405 Dufour, E., & Riaublanc, A. (1997). Potentiality of spectroscopic methods for the characterisation of dairy
406 products. i. front-face fluorescence study of raw, heated and homogenised milks. *Le Lait, 77*,
407 657-670.
408 Farrés, M., Platikanov, S., Tsakovski, S., & Tauler, R. (2015). Comparison of the variable importance in
409 projection (VIP) and of the selectivity ratio (SR) methods for variable selection and
410 interpretation. *Journal of Chemometrics, 29*, 528-536.
411 Foegeding, E. A., Brown, J., Drake, M., & Daubert, C. R. (2003). Sensory and mechanical aspects of
412 cheese texture. *International Dairy Journal, 13*, 585-591.
413 Fox, J. B. Jr., & Thayer, D. W. (1998). Radical oxidation of riboflavin. *International Journal for Vitamin*
414 *and Nutrition Research, 68*, 174-180.
415 Fujita, K., Tsuta, M., Kokawa, M., & Sugiyama, J. (2010). Detection of deoxynivalenol using
416 fluorescence excitation-emission matrix. *Food and Bioprocess Technology, 3*, 922-927.
417 Garimella Purna, S. K., Prow, L. A., & Metzger, L. E. (2005). Utilization of front-face fluorescence
418 spectroscopy for analysis of process cheese functionality. *Journal of Dairy Science, 88*, 470-477.
419 Guinee, T. P., Caric, M., & Kalab, M. (2004). Pasteurized processed cheese and substitute/imitation
420 cheese products. *Cheese: Chemistry, Physics and Microbiology, 2*, 349-394.
421 Guinee, T. P., & Kilcawley, K. N. (2004). Cheese as an ingredient. *Cheese: Chemistry, Physics and*
422 *Microbiology 2*, 395-428.
423 Henry, R. C., Park, E. S., & Spiegelman, C. H. (1999). Comparing a new algorithm with the classic
424 methods for estimating the number of factors. *Chemometrics and Intelligent Laboratory Systems,*
425 *48*, 91-97.
426 Herbert, S., Riou, N. M., Devaux, M. F., Riaublanc, A., Bouchet, B., Gallant, D. J., et al. (2000).

427 Monitoring the identity and the structure of soft cheeses by fluorescence spectroscopy. *Le Lait,*
428 *80*, 621-634.
429 ISO/IDF. (2002). *Milk and milk products: Determination of nitrogen content: Routine method using*
430 *combustion according to the Dumas principle. 185:2002.* Brussels, Belgium: International Dairy
431 Federation.
432 ISO/IDF. (2004a). *Cheese and processed cheese: Determination of the total solids content (Reference*
433 *method). 4:2004.* Brussels, Belgium: International Dairy Federation.
434 ISO/IDF. (2004b). *Cheese and processed cheese products: Determination of fat content: Gravimetric*
435 *method (Reference method). 5:2004.* Brussels, Belgium: International Dairy Federation.
436 Kapoor, R., & Metzger, L. E. (2008). Process cheese: scientific and technological aspects - a review.
437 *Comprehensive Reviews in Food Science and Food Safety, 7*, 194-214.
438 Karoui, R., & Blecker, C. (2011). Fluorescence spectroscopy measurement for quality assessment of food
439 systems - a review. *Food and Bioprocess Technology, 4*, 364-386.
440 Karoui, R., & Dufour, E. (2006). Prediction of the rheology parameters of ripened semi-hard cheeses
441 using fluorescence spectra in the UV and visible ranges recorded at a young stage. *International*
442 *Dairy Journal, 16*, 1490-1497.
443 Karoui, R., Dufour, E., & De Baerdemaeker, J. (2006). Common components and specific weights
444 analysis: a tool for monitoring the molecular structure of semi-hard cheese throughout ripening.
445 *Analytica Chimica Acta, 572*, 125-133.
446 Karoui, R., Mazerolles, G., & Dufour, E. (2003). Spectroscopic techniques coupled with chemometric
447 tools for structure and texture determinations in dairy products. *International Dairy Journal, 13*,
448 607-620.
449 Kikugawa, K., & Beppu, M. (1987). Involvement of lipid oxidation products in the formation of
450 fluorescent and cross-linked proteins. *Chemistry and Physics of Lipids, 44*, 277-296.

Kikugawa, K., Takayanagi, K., & Watanabe, S. (1985). Polylysines modified with malonaldehyde, hydroperoxylinoleic acid and monofunctional aldehydes. *Chemical & Pharmaceutical Bulletin, 33*, 5437-5444.

Kokawa, M., Ikegami, S., Chiba, A., Koishihara, H., Trivittayasil, V., Tsuta, M., et al. (2015). Measuring cheese maturation with the fluorescence fingerprint. *Food Science and Technology Research, 21*, 549-555.

Kulmyrzaev, A., Dufour, E., Noël, Y., Hanafi, M., Karoui, R., Qannari, E. M., et al. (2005). Investigation at the molecular level of soft cheese quality and ripening by infrared and fluorescence spectroscopies and chemometrics - relationships with rheology properties. *International Dairy Journal, 15*, 669-678.

Kulmyrzaev, A. A., Karoui, R., De Baerdemaeker, J., & Dufour, E. (2007). Infrared and fluorescence spectroscopic techniques for the determination of nutritional constituents in foods. *International Journal of Food Properties, 10*, 299-320.

Lacotte, P., Gomez, F., Bardeau, F., Muller, S., Acharid, A., Quervel, X., et al. (2015). Amaltheys: A fluorescence-based analyzer to assess cheese milk denatured whey proteins. *Journal of Dairy Science, 98*, 6668-6677.

Lebecque, A., Laguet, A., Devaux, M. F., & Dufour, É. (2001). Delineation of the texture of salers cheese by sensory analysis and physical methods. *Le Lait, 81*, 609-624.

Lee, C.H., Imoto, E.M., & Rha, C. (1978). Evaluation of cheese texture. *Journal of Food Science, 43*, 1600-1605.

Liu, Z., Sajith Babu, K., Coutouly, A., Allouche, F., & Amamcharla, J. K. (2016). Prediction of intact casein in cheese by using Amaltheys: a front-face fluorescence analyzer. *Journal of Animal Science, 94*, 250.

Mazerolles, G., Devaux, M. F., Duboz, G., Duployer, M. H., Riou, N. M., & Dufour, E. (2001). Infrared

and fluorescence spectroscopy for monitoring protein structure and interaction changes during cheese ripening. *Le Lait, 81*, 509-527.

Mehmood, T., Liland, K. H., Snipen, L., & Sæbø, S. (2012). A review of variable selection methods in partial least squares regression. *Chemometrics and Intelligent Laboratory Systems, 118*, 62-69.

Mita Mala, D., Yoshimura, M., Kawasaki, S., Tsuta, M., Kokawa, M., Trivittayasil, V., et al. (2016). Fiber optics fluorescence fingerprint measurement for aerobic plate count prediction on sliced beef surface. *LWT - Food Science and Technology, 68*, 14-20.

Mizuno, R., & Ichihashi, N. (2007). Characterization of two types of cheddar cheese as ingredients for processed cheese. *Nippon Shokuhin Kagaku Kogaku Kaishi, 54*, 395-400.

Morales, F. J., Romero, C., & Jiménez-Pérez, S. (1996). Fluorescence associated with Maillard reaction in milk and milk-resembling systems. *Food Chemistry, 57*, 423-428.

Morita, A., Araki, T., Ikegami, S., Okaue, M., Sumi, M., Ueda, R., et al. (2015). Coupled stepwise PLS-VIP and ANN modeling for identifying and ranking aroma components contributing to the palatability of cheddar cheese. *Food Science and Technology Research, 21*, 175-186.

Muir, D. D. (2010). The grading and sensory profiling of cheese. In B. A. Law, A. Y. Tamime (Eds.). *Technology of Cheesemaking* (pp. 440-474): Wiley-Blackwell.

Nakazawa, Y., & Hosono, A. (1989). *Recent advances in cheese science and technology*. New Food Industry.

Nawrocka, A., & Lamorska, J. (2013). Determination of food quality by using spectroscopic methods. In S. Grundas & A. Stepniewski (Eds.), *Advances in Agrophysical Research* (Ch. 14). InTech.

O'Callaghan, D. J., & Guinee, T. P. (2004). Rheology and texture of cheese. In P. F. Fox, P. L. H. McSweeney, T. M. Cogan & T. P. Guinee (Eds.), *Cheese: Chemistry, Physics and Microbiology* (Vol. 1, pp. 511-540). London: Academic Press.

Ozbekova, Z., & Kulmyrzaev, A. (2017). Fluorescence spectroscopy as a non destructive method to

predict rheological characteristics of tilsit cheese. *Journal of Food Engineering, 210*, 42-49.

Rajalahti, T., Arneberg, R., Berven, F. S., Myhr, K. M., Ulvik, R. J., & Kvalheim, O. M. (2009). Biomarker discovery in mass spectral profiles by means of selectivity ratio plot. *Chemometrics and Intelligent Laboratory Systems, 95*, 35-48.

Sádecká, J., & Tóthová, J. (2007). Fluorescence spectroscopy and chemometrics in the food classification - a review. *Czech Journal of Food Sciences, 25*, 159-173.

Schwietzke, U., Schwarzenbolz, U., & Henle, T. (2009). Influence of cheese type and maturation time on the early Maillard reaction in cheese. *Czech Journal of Food Sciences, 27*, S140-S142.

Spanneberg, R., Salzwedel, G., & Glomb, M. A. (2012). Formation of early and advanced Maillard reaction products correlates to the ripening of cheese. *Journal of Agricultural and Food Chemistry, 60,* 600-607.

Stapelfeldt, H., & Skibsted, L. H. (1994). Modification of β–lactoglobulin by aliphatic aldehydes in aqueous solution. *Journal of Dairy Research, 61*, 209-219.

Tamime, A. Y. (2011). *Processed cheese and analogues* (Vol. 16). John Wiley & Sons.

Veberg, A., Olsen, E., Nilsen, A. N., & Wold, J. P. (2007). Front-face fluorescence measurement of photosensitizers and lipid oxidation products during the photooxidation of butter. *Journal of Dairy Science, 90*, 2189-2199.

Veberg, A., Vogt, G., & Wold, J. P. (2006). Fluorescence in aldehyde model systems related to lipid oxidation. *LWT - Food Science and Technology, 39*, 562-570.

Xiong, R., Meullenet, J. F., Hankins, J. A., & Chung, W. K. (2002). Relationship between sensory and instrumental hardness of commercial cheeses. *Journal of Food Science, 67*, 877-883.

Yamaki, S., Kato, T., & Kikugawa, K. (1992). Characteristics of fluorescence formed by the reaction of proteins with unsaturated aldehydes, possible degradation products of lipid radicals. *Chemical and Pharmaceutical Bulletin, 40*, 2138-2142.

Yoshimura, M., Sugiyama, J., Tsuta, M., Fujita, K., Shibata, M., Kokawa, M., et al. (2014). Prediction of aerobic plate count on beef surface using fluorescence fingerprint. *Food and Bioprocess Technology, 7*, 1496-1504.

527 **Figure legends**

528

529 **Fig. 1**. Examples of fluorescence fingerprints (FFs) of Cheddar cheese surfaces obtained using optical

530 fiber in the range of normal intensities (0–6000 intensity (a.u.)).

531

532 **Fig. 2**. Predicted vs measured cheese body measurements obtained by PLSR calibration. Bold lines show

533 y = x.

534

535 **Fig. 3**. Predicted vs measured cheese body measurements obtained by PLSR validation. Bold lines show

536 y = x.

537

538 **Fig. 4**. Contour plot of each score in the PLS model: (a) VIP, (b) SR, (c) regression vector.

539

540 **Fig. 5**. Fluorescence emission spectra color-coded by cheese body measurement at excitation wavelengths

541 of (a) 340 nm, (b) 385 nm, and (c) 305 nm.

Table 1

Physico-chemical compositions of the 10 Cheddar cheeses.

Cheese samples	Age at measuments (days) 1st	2nd	3rd	Storage temperature (^{o}C)	pH	Dry matter (g/100g^{-1})	Fat (g/100g^{-1})	Protein (g/100g^{-1})	Salt (g/100g^{-1})
1	231	269	318	-2	5.42	67.4	34.9	27.5	1.9
2	132	170	219	-2	5.40	67.3	34.7	27.4	2.0
3	111	149	198	-2	5.47	67.6	34.6	27.5	2.1
4	231	269	318	5	5.48	67.7	34.9	27.3	1.9
5	132	170	219	5	5.43	67.9	35.3	27.7	2.2
6	231	269	318	10	5.39	67.7	35.5	27.2	1.9
7	203	241	290	10	5.52	67.6	35.5	27.4	1.9
8	231	269	318	15	5.55	68.1	35.6	27.2	2.1
9	203	241	290	15	5.47	68.0	35.1	27.7	2.1
10	132	170	219	15	5.41	67.6	35.3	27.5	2.1

Table 2
Results of PLS regression for four pretreatment methods.

Pretreatment	LVs	RMSECV	R^2CV	R^2C *	R^2P	RMCEP
mean center	3	0.456	0.787	0.800	0.826	0.436
normalize + mean center	3	0.456	0.787	0.808	0.747	0.515
autoscale	3	0.493	0.757	0.822	0.787	0.470
normalize + autoscale	2	0.482	0.762	0.787	0.739	0.519

* The coefficients of determination for calibration.

Figure

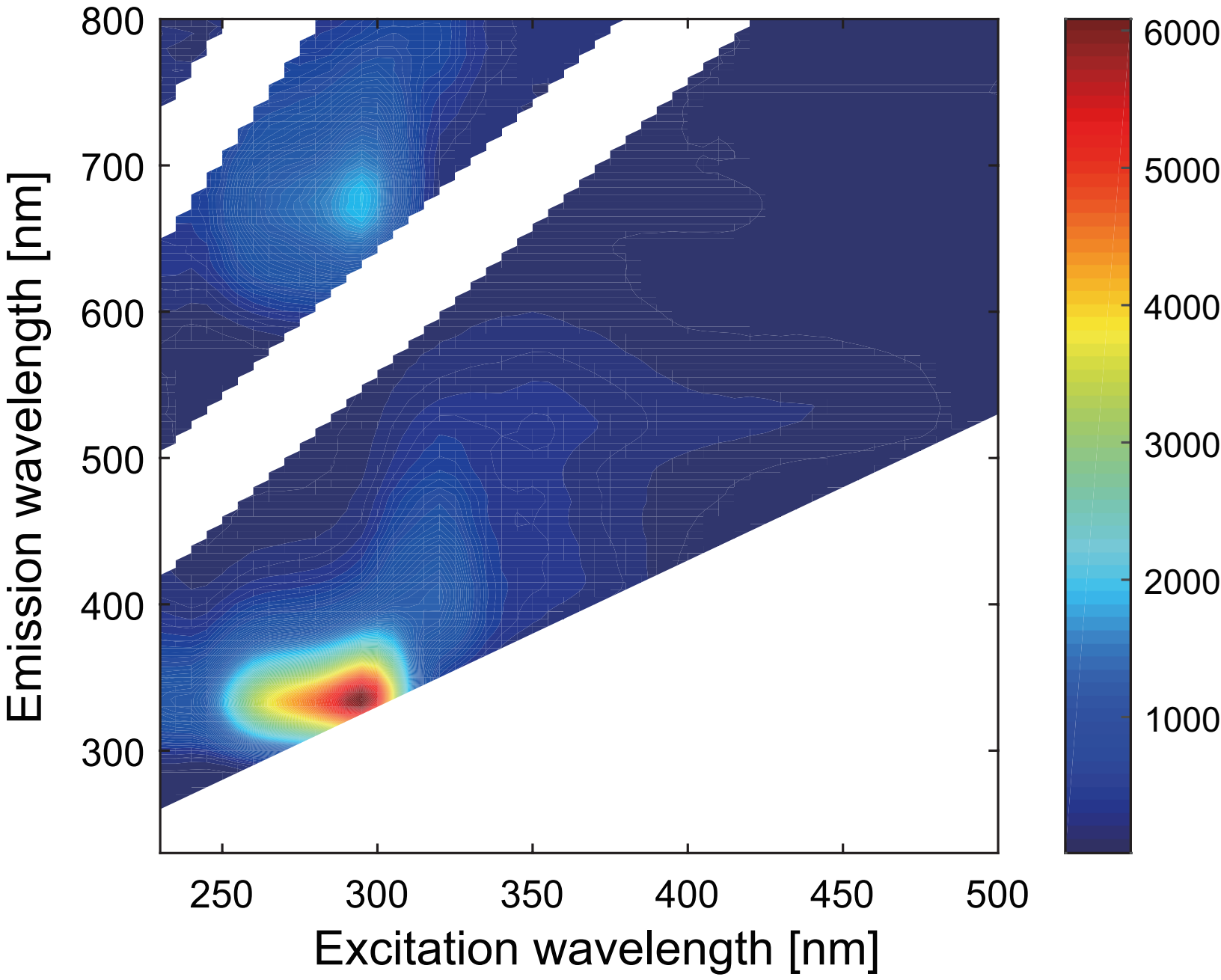
800
700
600
500
400
300
Emission wavelength [nm]
250
300
350
400
450
500
Excitation wavelength [nm]
6000
5000
4000
3000
2000
1000

Figure

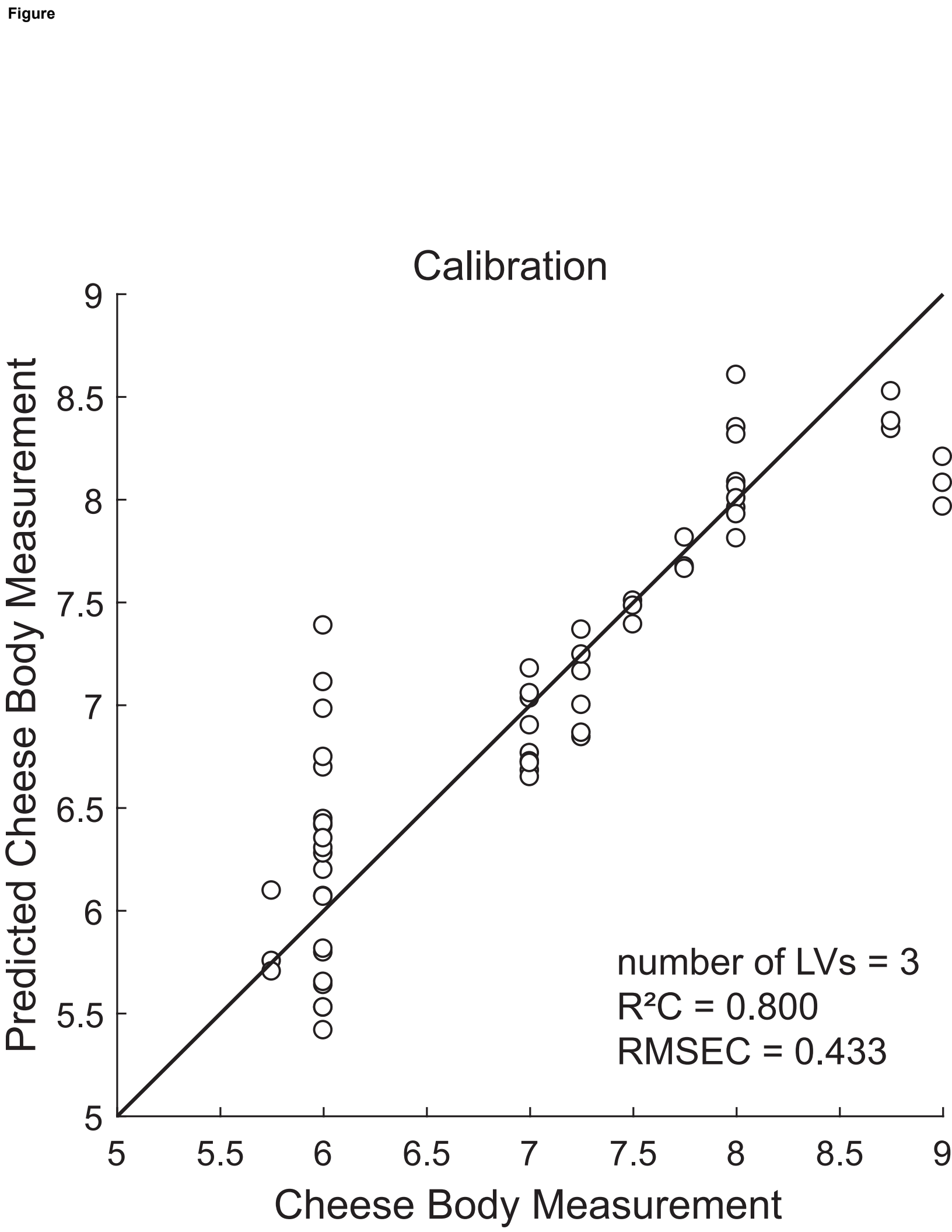
Calibration
Predicted Cheese Body Measurement
Cheese Body Measurement
number of LVs = 3
R²C = 0.800
RMSEC = 0.433
5
5.5
6
6.5
7
7.5
8
8.5
9

Figure

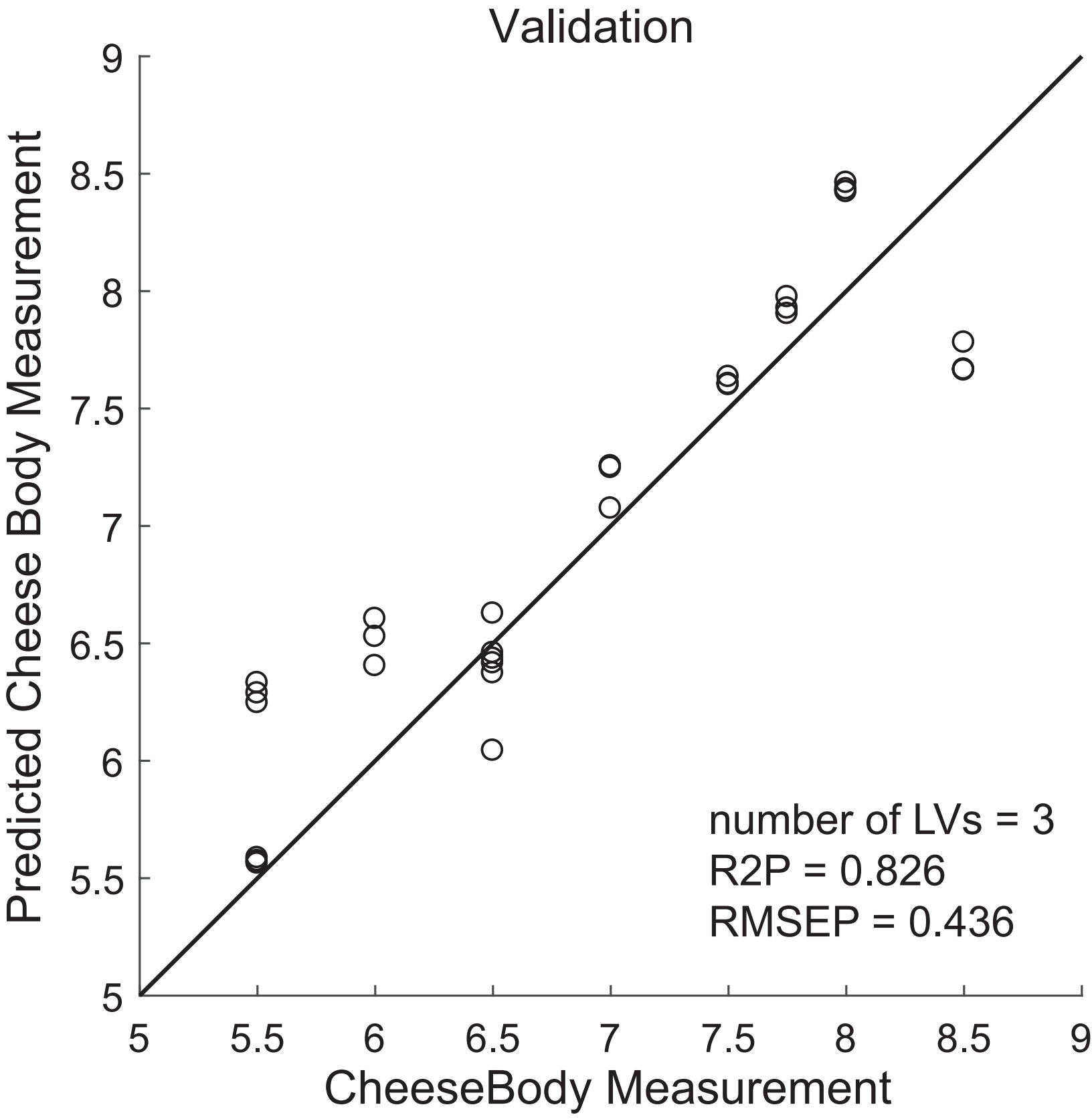
Validation
Predicted Cheese Body Measurement
CheeseBody Measurement
number of LVs = 3
R2P = 0.826
RMSEP = 0.436
9
8.5
8
7.5
7
6.5
6
5.5
5
5
5.5
6
6.5
7
7.5
8
8.5
9

Figure

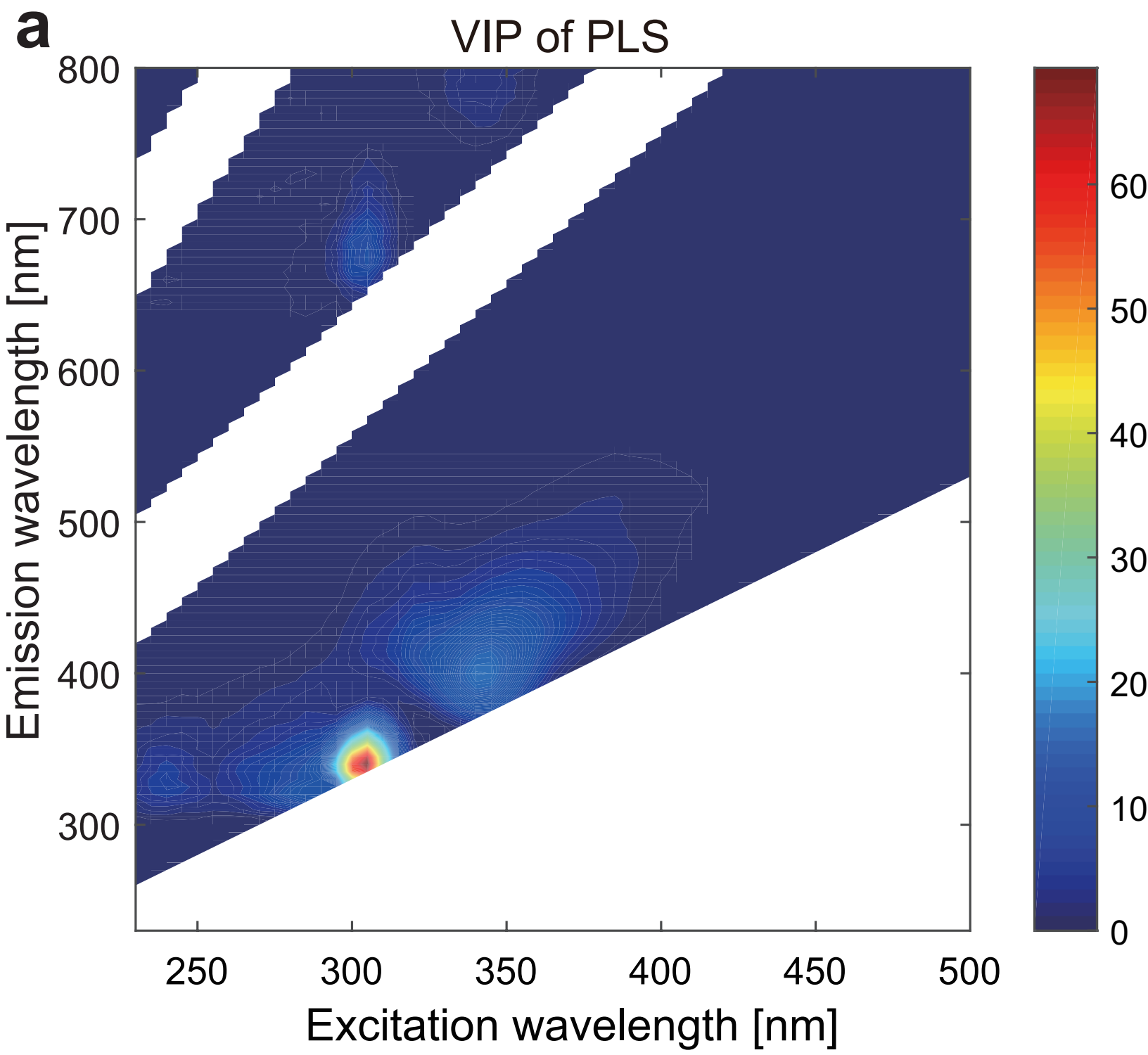
a
VIP of PLS
800
700
600
500
400
300
Emission wavelength [nm]
250
300
350
400
450
500
Excitation wavelength [nm]
60
50
40
30
20
10
0

Figure

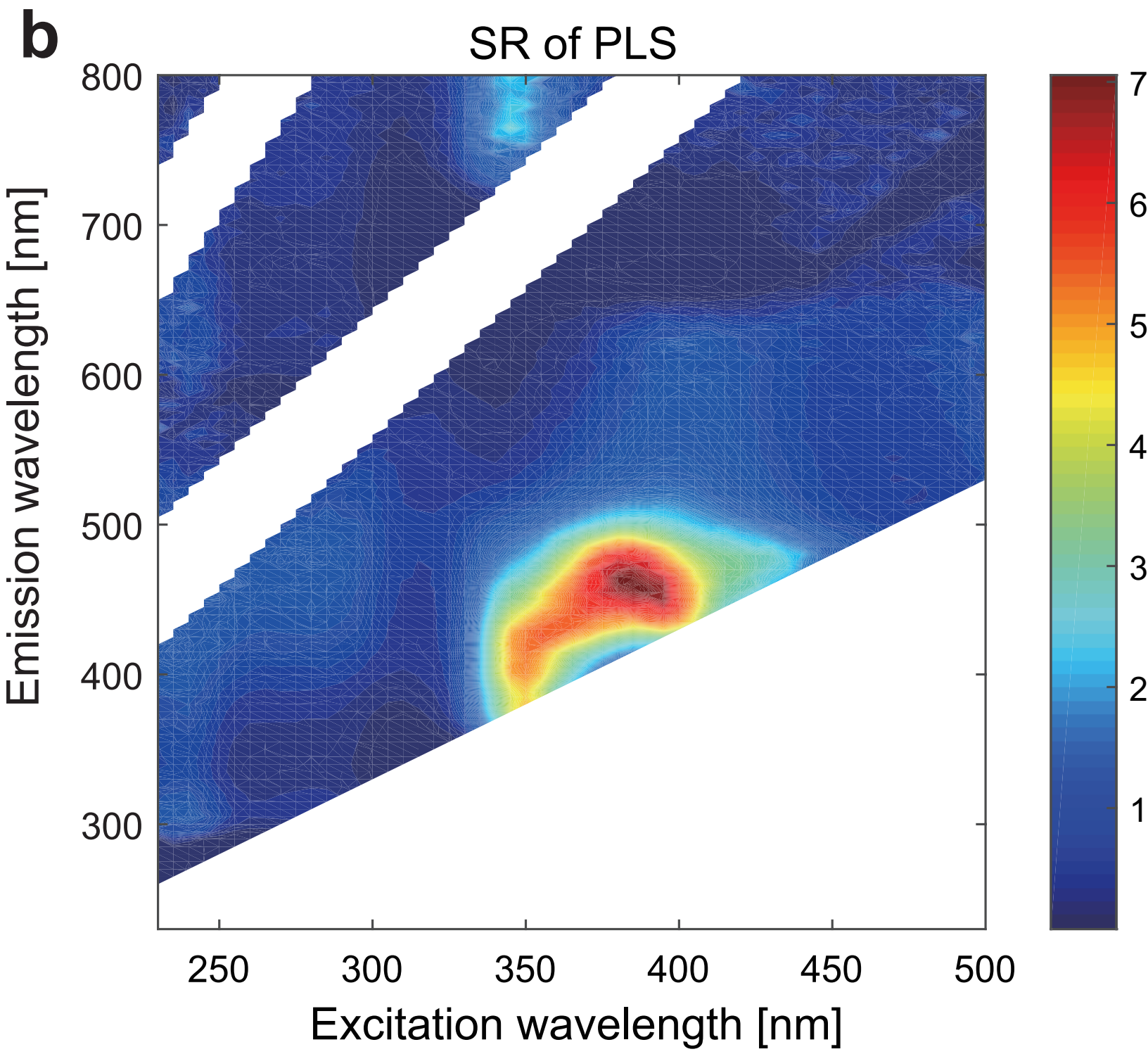
b
SR of PLS
800
700
600
500
400
300
Emission wavelength [nm]
250
300
350
400
450
500
Excitation wavelength [nm]
7
6
5
4
3
2
1

Figure

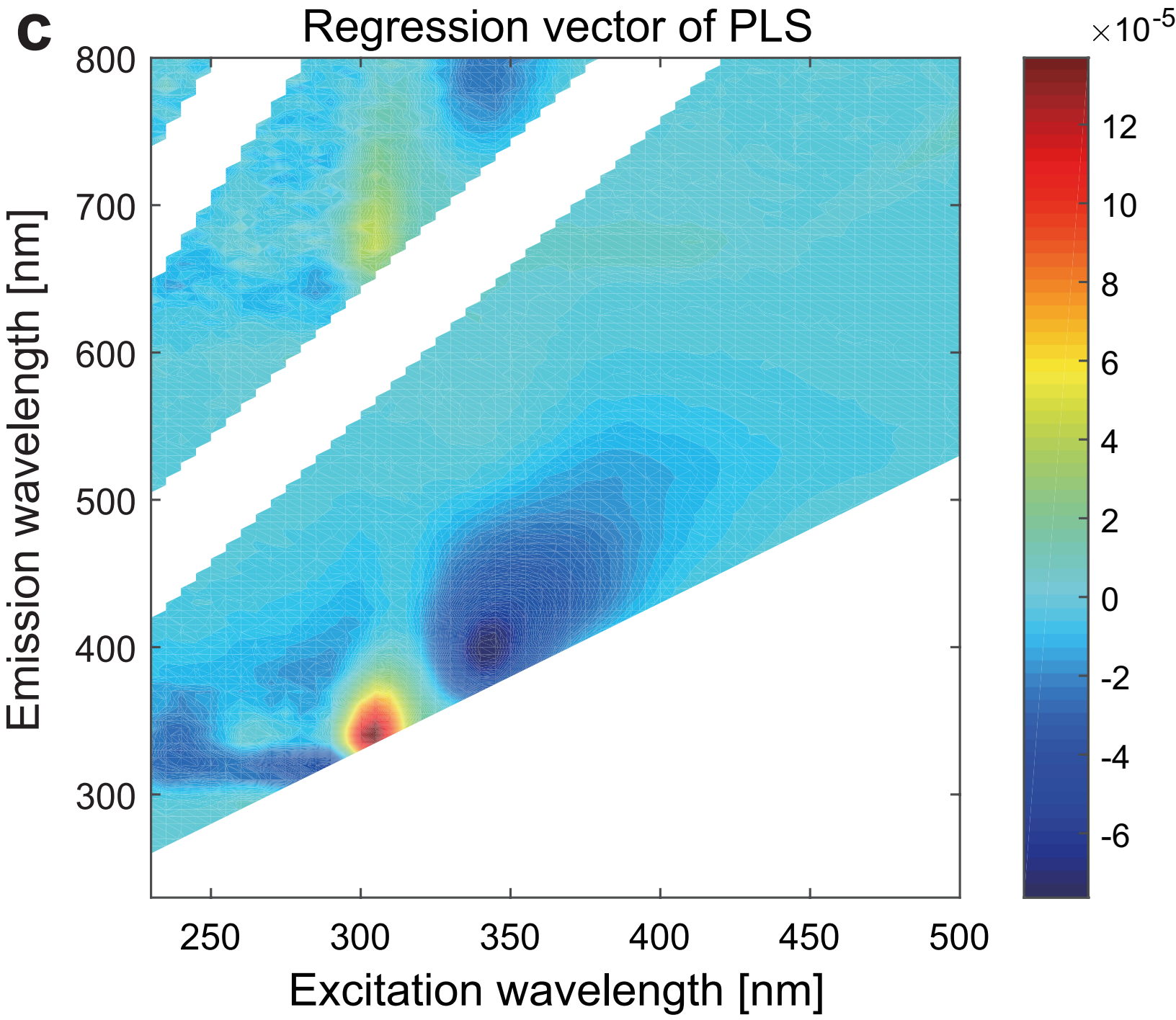
c
Regression vector of PLS
×10-5
12
10
8
6
4
2
0
-2
-4
-6
800
700
600
500
400
300
Emission wavelength [nm]
250
300
350
400
450
500
Excitation wavelength [nm]

Figure

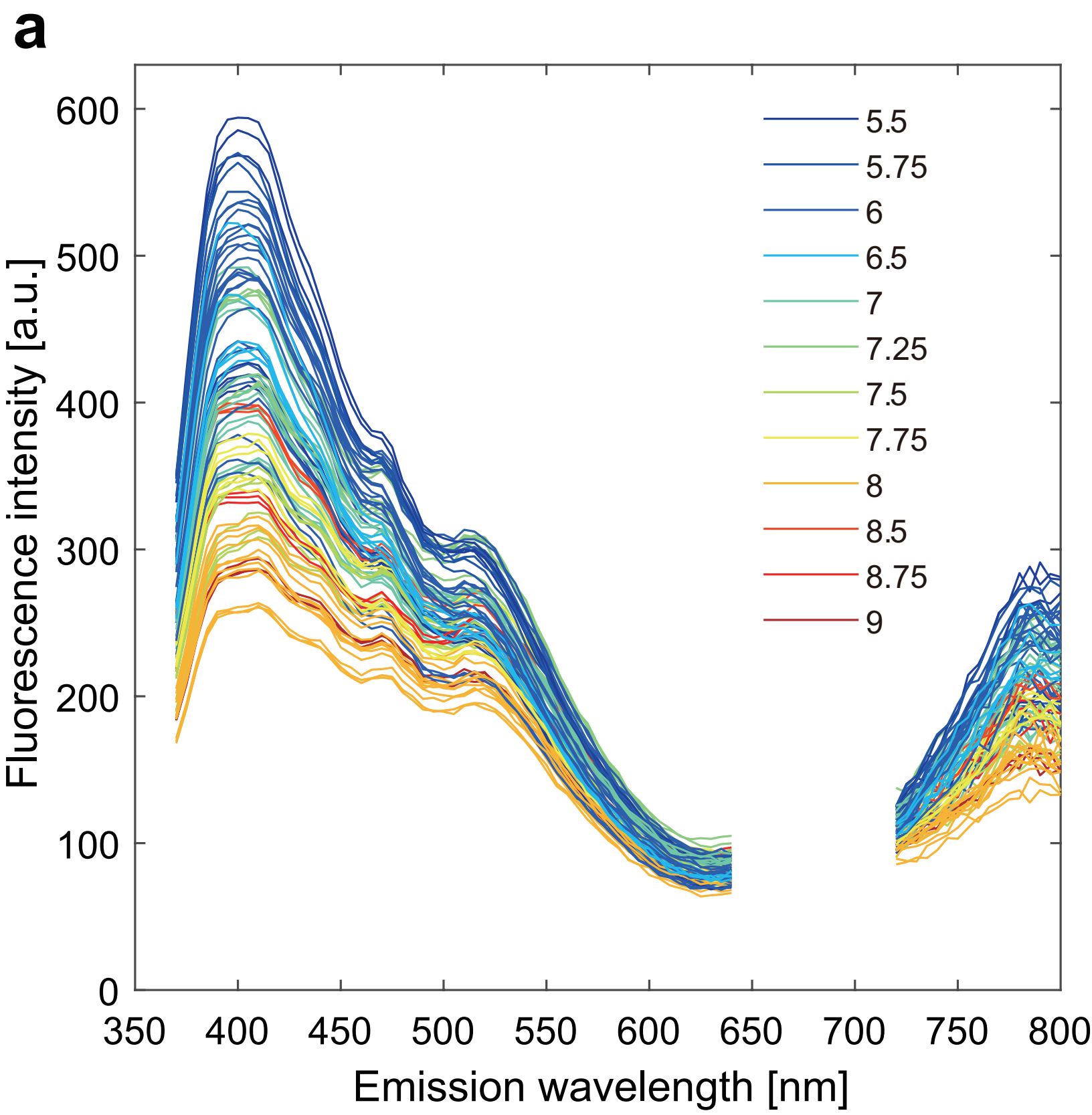
a
Fluorescence intensity [a.u.]
0
100
200
300
400
500
600
350
400
450
500
550
600
650
700
750
800
Emission wavelength [nm]
5.5
5.75
6
6.5
7
7.25
7.5
7.75
8
8.5
8.75
9

Figure

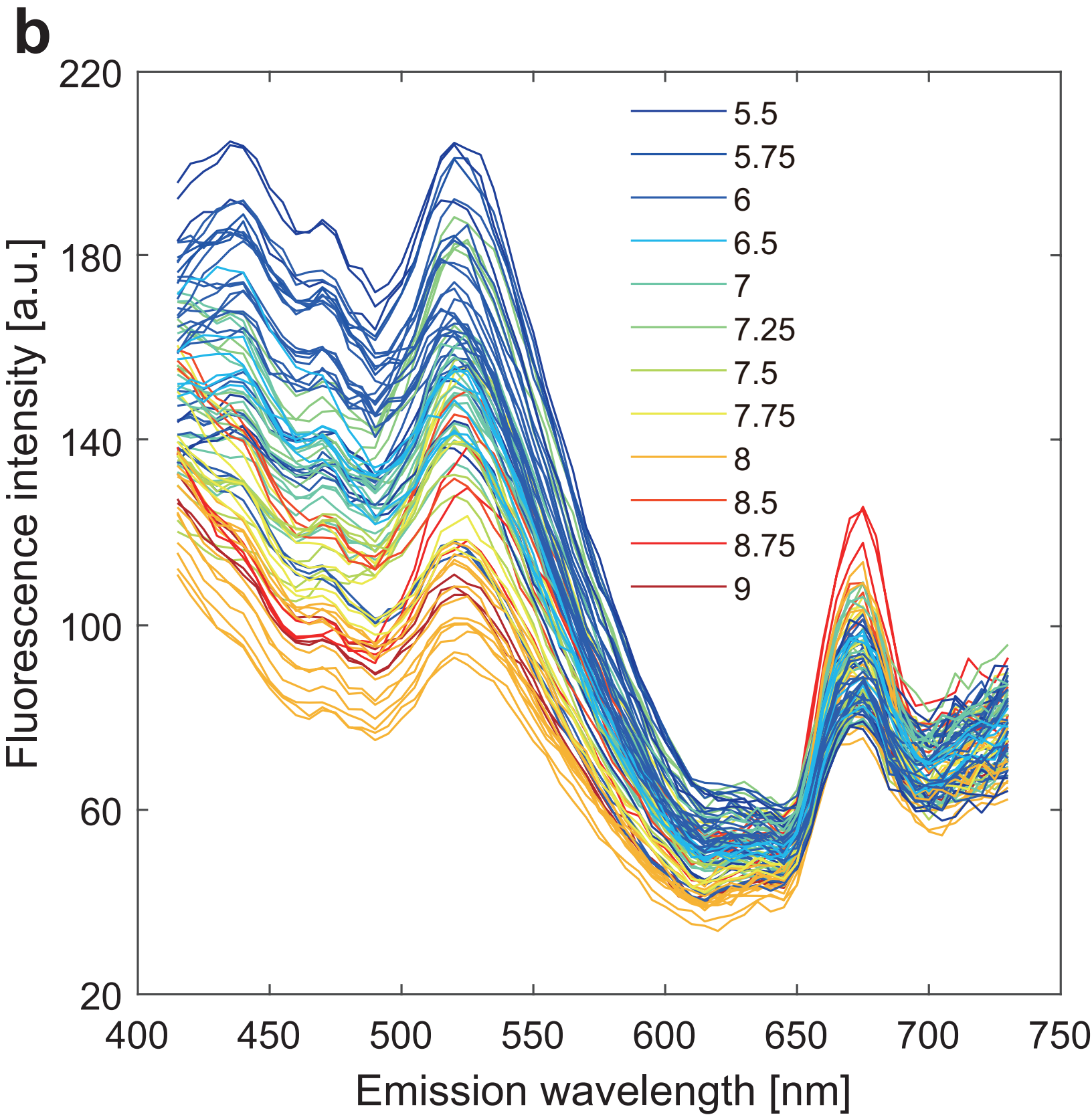
b
220
180
140
100
60
20
Fluorescence intensity [a.u.]
400
450
500
550
600
650
700
750
Emission wavelength [nm]
5.5
5.75
6
6.5
7
7.25
7.5
7.75
8
8.5
8.75
9

Figure

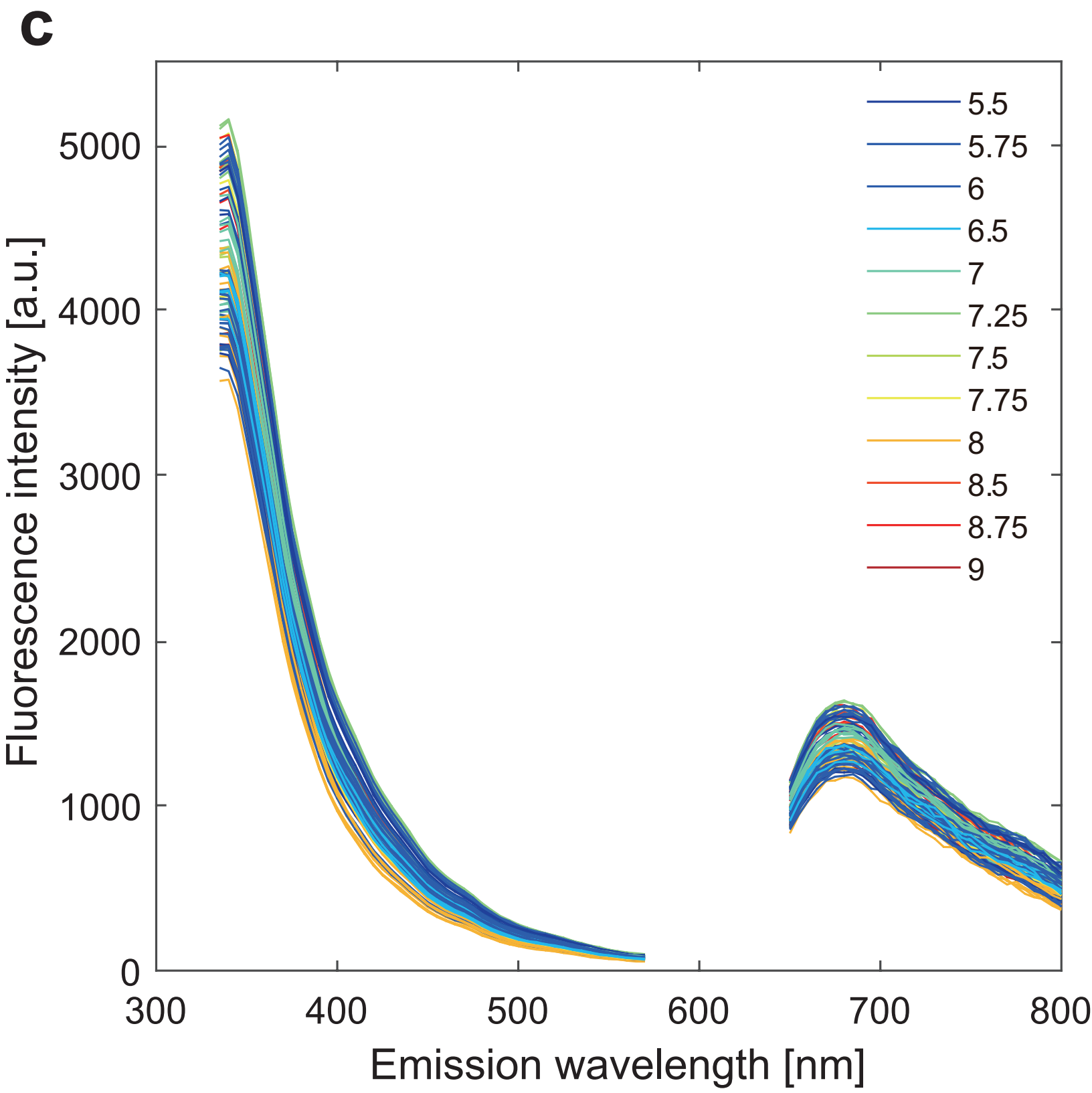
c
5000
4000
3000
2000
1000
0
Fluorescence intensity [a.u.]
300
400
500
600
700
800
Emission wavelength [nm]
5.5
5.75
6
6.5
7
7.25
7.5
7.75
8
8.5
8.75
9